The effect of gas accretion on the radial abundance profiles of galaxies

F. Collacchioni[1,2], C.D.P. Lagos[3,4], P.D. Mitchell[5,6] & S.A. Cora[1,2]

[1] *Instituto de Astrofísica de La Plata, CONICET–UNLP, Argentina*
[2] *Facultad de Ciencias Astronómicas y Geofísicas, UNLP, Argentina*
[3] *International Centre for Radio Astronomy Research, Perth, Australia*
[4] *The Cosmic Dawn Center, University of Copenhagen, Copenhagen, Denmark*
[5] *Leiden Observatory, Leiden University, Leiden, The Netherlands*
[6] *Université Claude Berbard Lyon 1, Lyon, France*

Contact / fcollacchioni@fcaglp.unlp.edu.ar

Resumen / El advenimiento de la espectroscopía de campo integral ha permitido la caracterización de los perfiles radiales de metalicidad (RMP, por sus siglas en inglés) de miles de galaxias locales y de varias docenas a alto corrimiento al rojo. Esto ha ayudado a encontrar que los gradientes radiales cambian como función de la masa estelar y la tasa de formación estelar y, sorprendentemente, se aplanan en las regiones externas de las galaxias. Estudiamos las causas físicas de estas tendencias usando la simulación cosmológica EAGLE y nos enfocamos especialmente en galaxias centrales de $M_\star \geq 10^{10}$ $M_\odot$. Encontramos una clara correlación entre la tasa de gas acretado ($\dot{M}_{\rm accr}$) y el gradiente interno (dentro de un radio efectivo) del RMP, de manera que galaxias con mayor $\dot{M}_{\rm accr}$ están asociadas a gradientes más grandes. Se encuentra que el gradiente de los RMPs presenta una dependencia más fuerte con $\dot{M}_{\rm accr}$ que con la masa estelar o la tasa de formación estelar, sugiriendo que el gas acretado es un trazador más fundamental de los RMPs de galaxias. Estas tendencias están presentes en la simulación para todo el rango de corrimiento al rojo estudiado aquí ($z \leq 1$).

Abstract / The advent of integral field spectroscopy has allowed the characterization of radial gas metallicity profiles (RMPs) in many thousands of local galaxies and several dozens at high redshift. This has helped in finding that radial gradients change as a function of stellar mass and star formation rate and, more surprisingly, that they flatten in the outskirts of galaxies. We study the physical causes of these trends using the state-of-the-art hydrodynamic simulation EAGLE and focusing specifically on central galaxies of $M_\star \geq 10^{10}$ $M_\odot$. We find clear correlations between the gas accretion rate ($\dot{M}_{\rm accr}$) and the internal (within an effective radius) gradient of the RMP, in a way that higher $\dot{M}_{\rm accr}$ are associated to larger gradients. The gradient of the RMPs is found to depend more strongly on $\dot{M}_{\rm accr}$ than on stellar mass or star formation rate, suggesting the gas accretion to be a more fundamental driver of the RMP of galaxies. These trends are present in the simulation for the full range of redshift studied here ($z \leq 1$).

Keywords / methods: numerical — galaxies: evolution — galaxies: formation

1. Introduction

Integral field spectroscopy (e.g. Sánchez et al., 2012; Carton et al., 2018) provides spatially resolved information that greatly contributed to advance our understandig of galaxy formation and evolution. In particular, the analysis of radial metallicity profiles (RMPs) is essential to understand how the galaxy chemical enrichment evolves, since it correlates the metal abundance of the gas-phase of a galaxy as a function of the distance to its centre.

There is still an open debate on the shape of the RMPs (in particular concerning their behaviour with radius) and what properties are involved in its shaping, encompassing both observational and theoretical arguments (see Collacchioni et al. 2019 for a brief summary). In this sense, gas accretion plays an important role, since it can dilute the metals present in the galaxy's gas, and it can also trigger star formation, which will then pollute the interstellar medium with the material formed through nucleosinthesis (Perez et al., 2011; Finlator, 2017). However, due to the observational limitations to measure this gas accretion, we use a cosmological hydrodynamic simulation with the aim to understand the effect of gas accretion onto the RMPs and to determine the traces it leaves.

2. Methodology

We use a hydrodynamical simulation from the Evolution and Assembly of GaLaxies and their Environments (EAGLE) project[⋆]. EAGLE follows the evolution of dark matter and baryons, consistent with a flat ΛCDM cosmology characterised by the Planck Collaboration et al. (2014) parameters. The subgrid physical models are detailed in Schaye et al. (2015) and Crain et al.

[⋆] `http://icc.dur.ac.uk/Eagle/`

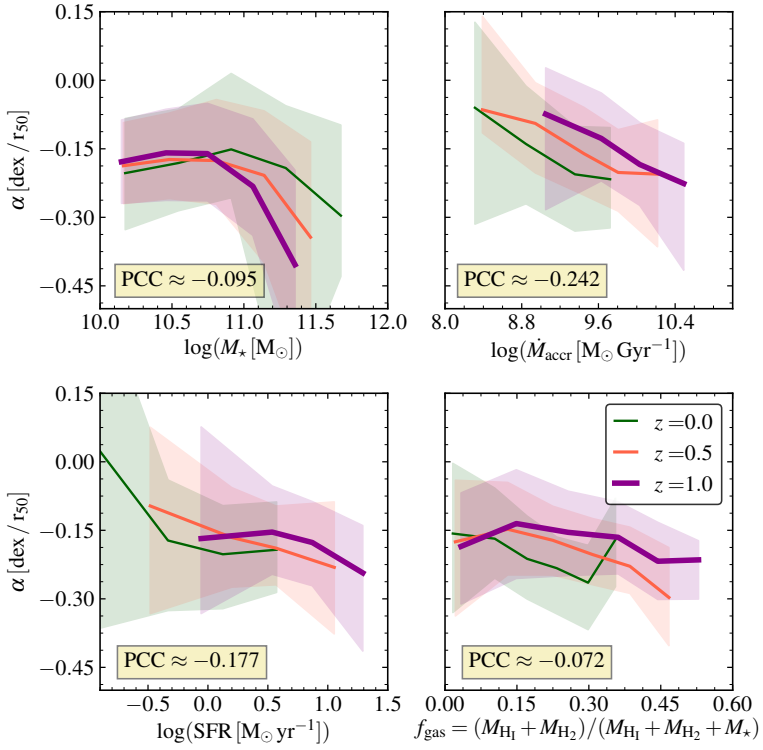

Figure 1: Gradient of the RMP, α, as a function of stellar mass (top left panel), $\dot{M}_{\rm accr}$ (top right panel), SFR (bottom left panel), and $f_{\rm gas}$ (bottom right panel). Galaxy gradients are calculated for radius of $r \leq {\rm r}_{50}$, where r_{50} is the effective radius. Solid lines depict median values of the relations, and shadows show the 1σ dispersion. Redshifts $z = 0.0$, $z = 0.5$ and $z = 1.0$ are represented by colours green, orange and violet, respectively. The mean temporal value of the Pearson Correlation Coefficient is shown for each relation. Statistically, α is more correlated with $\dot{M}_{\rm accr}$.

(2015), and the reader can refer to The EAGLE team (2017) for the description of the public release of particle data. The simulation we used implements the so-called reference model (100^3 cMpc^3 volume).

We use a particle tracking methodogy (Neistein et al., 2012) to calculate the gas accretion rate, $\dot{M}_{\rm accr}$. The gas particles that compose the accreting gas mass of a given subhalo are those that fulfil the conditions of: *i)* being classified as star-forming (SF) at a given snapshot; *ii)* being bound to the main progenitor at the previous snapshot; and *iii)* being a not star-forming (NSF) particle at the previous snapshot. In this sense, we study the gas that changes its state from NSF to SF in the same subhalo (i.e., an smooth accretion that triggers star formation). Dividing the accretion gas mass by the time interval between snapshots we obtain the $\dot{M}_{\rm accr}$.

We estimate the metallicity whithin spherical shells centred at the potencial centre of each galaxy as

$$Z = \frac{M_{\rm metals}}{M_{\rm H} + M_{\rm He} + M_{\rm metals}}, \qquad (1)$$

where $M_{\rm H}$, $M_{\rm He}$ and $M_{\rm metals}$ are the masses of hydrogen, helium and metals of the SF gas particles, respectively (see Collacchioni et al. 2019 for more detail). Our sample selection includes central, star-forming galaxies with $M_\star \geq 10^{10}$ M$_\odot$ (cut due to the simulation resolution).

3. Results

Fig. 1 shows the gradient of the RMP, α, as a function of $M_\star$ (top left panel), $\dot{M}_{\rm accr}$ (top right panel), star formation rate (SFR, bottom left panel) and gas fraction ($f_{\rm gas}$, bottom right panel)**. There is a common trend for all these properties (except maybe $f_{\rm gas}$) that α decreases when the value of the properties increases. This is also seen at all redshifts considered ($z \leq 1$). We calculate the Pearson Correlation Coefficient (PCC) to measure which of these four properties is more statistically fundamental in the change of α, as it is shown in each panel. We find that the $\dot{M}_{\rm accr}$ is more fundamental in changing the gradient than the other properties.

Since $M_\star$ shows an anti-correlation with α and it is also correlated with the other three properties, we eliminate its dependence by obtaining the residuals as

$$\Delta X = X - \bar{X}, \qquad (2)$$

where X can be $\log(\dot{M}_{\rm accr})$, $\log({\rm SFR})$, or $f_{\rm gas}$, and $\bar{X}$ is the median value of X in the relation $\log(M_\star)$-X. Fig. 2 shows the relations of $\Delta\alpha$ as a funtion of $\Delta\,[\log(\dot{M}_{\rm accr})]$ (left panel), of $\Delta\,[\log(SFR)]$ (middle panel), and of $\Delta f_{\rm gas}$ (right panel). For these relations we calculate the PCC and find that, even when eliminating the dependence on $M_\star$, the rate $\dot{M}_{\rm accr}$ still shows an anti-correlation with α and, being the property that exhibits

**All properties are calculated using star-forming particles.

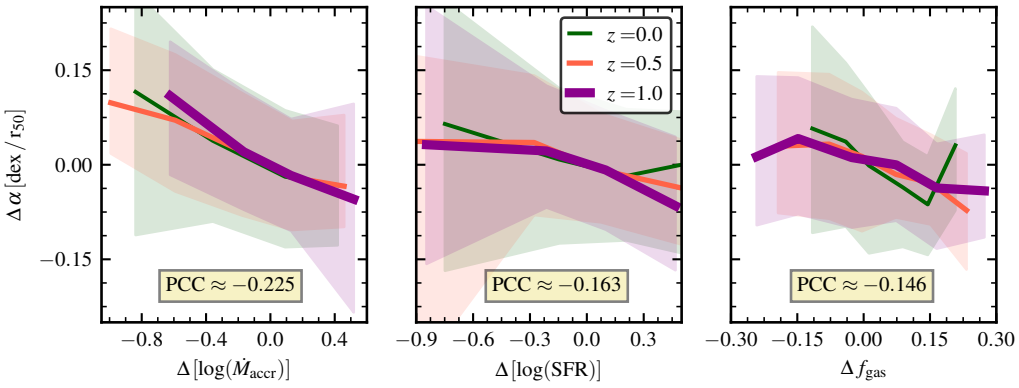

Figure 2: Residuals of the gradient of the RMP, $\Delta\alpha$, as a function of the residuals of the gas accretion rate ($\Delta\,[\log(\dot{M}_{\rm accr})]$, left panel), of SFR ($\Delta\,[\log(\rm SFR)]$, middle panel), and of the gas fraction ($\Delta\,f_{\rm gas}$, right panel). As in Fig. 1, galaxy gradients are calculated for radius of $r \leq \rm r_{50}$. Solid lines depict median values of the relations, and shadows show the 1σ dispersion. Redshifts $z = 0.0$, $z = 0.5$ and $z = 1.0$ are represented by colours green, orange and violet, respectively. The mean temporal value of the PCC is shown for each relation. Statistically, $\Delta\alpha$ is more correlated with $\Delta\,[\log(\dot{M}_{\rm accr})]$.

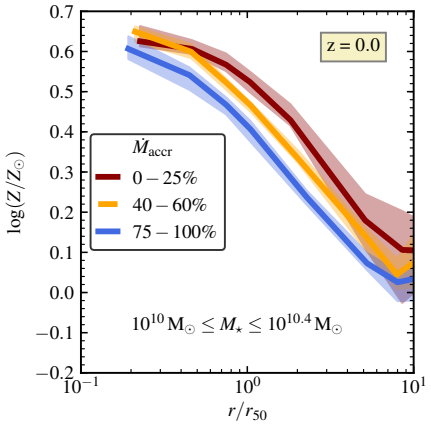

Figure 3: Median radial metallicity profiles for different values of $\dot{M}_{\rm accr}$ for galaxies with 10^{10} M$_\odot \leq M_\star \leq 10^{10.4}$ M$_\odot$ at $z = 0.0$. Lines depict median values, while shadows represent the 1σ dispersion. Galaxies with the 25% lowest values of $\dot{M}_{\rm accr}$ are shown in red, intermediate values of $\dot{M}_{\rm accr}$ (between 40% and 60%) are shown in yellow, and with the higher values of $\dot{M}_{\rm accr}$ ($\geq$ 75%) are shown in blue. This panel is an example of all the cuts made in stellar mass and redshift. Same results are obtained for all other cuts.

the strongest correlation with α.

Fig. 3 shows how the RMP changes when considering different values of $\dot{M}_{\rm accr}$. This is an example for a range of stellar mass (10^{10} M$_\odot \leq M_\star \leq 10^{10.4}$ M$_\odot$) and redshift ($z = 0.0$), but we find similar results for other cuts. When considering galaxies with higher values of $\dot{M}_{\rm accr}$ (blue line), the inner profile ($r \lesssim r_{50}$, where r_{50} is the radius in which the galaxy reaches 50% of its stellar mass) is the steepest one. On the other hand, when considering galaxies with lower values of $\dot{M}_{\rm accr}$ (red line), the profile becomes flatter.

4. Conclusions

We use the EAGLE reference cosmological simulation to study how gas accretion shapes and intervenes on the radial metallicity profile of galaxies. We investigate how the gradient of the RMP, α, changes with $M_\star$, $\dot{M}_{\rm accr}$, SFR and $f_{\rm gas}$, finding that $\dot{M}_{\rm accr}$ is the more fundamental driver of the RMPs. We check our results using the Pearson Correlation Coefficient. We conclude that galaxies with higher values of $\dot{M}_{\rm accr}$ present more negative gradients, while galaxies with lower values of $\dot{M}_{\rm accr}$ present flatter profiles.

Acknowledgements: We thank the referee for the constructive comments that improved this manuscript. We acknowledge the Local Organizer and Scientific Committees of the 61$^{\rm th}$ Meeting of the AAA. We acknowledge the Virgo Consortium for making their simulation data available. The EAGLE simulations were performed using the DiRAC-2 facility at Durham, managed by the ICC, and the PRACE facility Curie based in France at TGCC, CEA, Bruyèresle-Châtel. We acknoledge funding from Consejo Nacional de Investigaciones Científicas y Técnicas (CONICET, PIP-0387) and Universidad Nacional de La Plata (11-G150), Argentina. FC acknowledges CONICET and the Australian Endeavour programme for their supporting fellowships. CL acknowledges the Australian Research Council Centre of Excellence for All Sky Astrophysics in 3 Dimensions.

References

Carton D., et al., 2018, MNRAS, 478, 4293
Collacchioni F., et al., 2019, arXiv e-prints, arXiv:1910.05377
Crain R.A., et al., 2015, MNRAS, 450, 1937
Finlator K., 2017, A. Fox, R. Davé (Eds.), *Gas Accretion onto Galaxies*, *Astrophysics and Space Science Library*, vol. 430, 221
Neistein E., et al., 2012, MNRAS, 421, 3579
Perez J., Michel-Dansac L., Tissera P.B., 2011, MNRAS, 417, 580
Planck Collaboration, et al., 2014, A&A, 571, A1
Sánchez S.F., et al., 2012, A&A, 538, A8
Schaye J., et al., 2015, MNRAS, 446, 521
The EAGLE team, 2017, arXiv e-prints, arXiv:1706.09899